Multistage performance deterioration in n-type crystalline silicon photovoltaic modules undergoing potential-induced degradation

Yutaka Komatsu[1*], Seira Yamaguchi[1], Atsushi Masuda[2], and Keisuke Ohdaira[1]

[1]*Graduate School of Advanced Science and Technology, Japan Advanced Institute of Science and Technology (JAIST), Nomi, Ishikawa 923-1292, Japan*
[2]*Research Center for Photovoltaics, National Institute of Advanced Industrial Science and Technology (AIST), Tsukuba, Ibaraki 305-8568, Japan*

*Corresponding author
E-mail address: ohdaira@jaist.ac.jp

Abstract

This study addresses the behavior of n-type front-emitter (FE) crystalline-silicon (c-Si) photovoltaic (PV) modules in potential-induced degradation (PID) tests with a long duration of up to 20 days. By PID tests where a negative bias of −1000 V was applied at 85 °C to 20 × 20-mm^2-sized n-type FE c-Si PV cells in modules, the short-circuit current density (J_{sc}) and the open-circuit voltage (V_{oc}) started to be decreased within 10 s, and strongly saturates within approximately 120 s, resulting in a reduction in the maximum output power (P_{max}) and its saturation. After the saturation, all the parameters were almost unchanged until after 1 h. However, the fill factor (FF) then started to decrease and saturated again. After approximately 48 h, FF further decreased again, accompanied by a reduction in V_{oc}. The first degradation is known to be due to an increase in the surface recombination of minority carriers by the accumulation of additional positive charges in the front Si nitride (SiN_x) films. The second and third degradations may be due to significant increases in recombination in the space charge region. The enhancement in recombination in the space charge region may be due to additional defect levels of sodium (Na) introduced into the space charge region in the p–n junction. We also performed recovery tests by applying a positive bias of +1000 V. The module with the first degradation completely recovered its performance losses, and the module with the second degradation was almost completely recovered. On the contrary, the modules with the third degradation could not be recovered. These findings may improve the understanding of the reliability of n-type FE c-Si PV modules in large-scale PV systems.

Keywords: Potential-induced degradation; Device reliability; Performance deterioration; N-type crystalline silicon solar cell; Photovoltaic module

1. Introduction

Large-scale photovoltaic (PV) systems have been installed worldwide over the last decades. These large-scale PV systems can efficiently generate a large amount of electricity. However, there can be unfavorable potential differences between grounded frames and cells, which may lead to significant performance losses in deployed PV modules, so-called potential-induced degradation (PID) [1–4]. PID has been considered one of the most important reliability issues because PID can, in many cases, lead to large power losses in a relatively short time.

PID in conventional p-type crystalline-silicon (c-Si) PV modules has been studied in detail thus far [1–9]. The PID of p-type c-Si PV modules occurs only when they have negative electrical potential with respect to aluminum (Al) frames, and is characterized mainly by a reduction in the fill factor (FF) due to a decrease in the parallel resistance (R_p). In the case of conventional p-type c-Si PV modules, sodium (Na) can drift from the cover glass and/or contaminants at the interfaces between cells and encapsulants into the n-type emitters of cells, with assistance from an electric field, through their front Si nitride (SiN_x) antireflection/passivation films, which are known as excellent diffusion barriers against Na [10,11]. From the mechanistic aspect, Naumann et al. have studied PID in p-type c-Si PV modules, and have revealed that the shunting is caused by the formation of Na-decorated stacking faults penetrating the front n-type emitters [8,9].

n-type c-Si PV cells generally have higher efficiencies than p-type ones, since the capture cross-sections of many types of impurities for minority carriers in n-type c-Si, holes, are smaller than those for electrons, and longer minority-carrier lifetimes can be obtained [12]. From this reason, the market share of these n-type c-Si PV cells is expected to increase in the near future. To ensure the long-term stability and the reliability of the n-type c-Si modules, it is important to understand their possible degradation behaviors. However, there are relatively fewer previous studies on PID occurring in n-type c-Si PV modules [13–23]. Hara et al. have reported that n-type front-emitter (FE) c-Si PV modules suffer PID characterized by reductions in the short-circuit current density (J_{sc}) and the open-circuit voltage (V_{oc}) under a negative bias [16]. Bae et al. have experimentally demonstrated that the degradation is caused by an increase in fixed positive charges in the front passivation layer [19]. We have reported that the degradation saturates within quite a short time, for instance, several minutes [17]. However, detailed progression behavior after the saturation of the degradation has not been clarified. Although Barbato et al. have reported the degradation behavior of n-type c-Si PV modules in PID tests with a long duration of up to 55 h [20], their PID tests were performed at a bias of up to −600 V, and different degradation phenomena may be found by performing severer PID tests.

In this study, we investigated the degradation behavior of n-type FE c-Si PV modules in PID tests with a long duration of up to 20 days, and found that the modules undergo three-stage degradations. We also investigated whether the degradation on each stage can

be recovered by applying a positive bias, and found that the degree of performance recovery depends on that of degradation. We attempted to explain possible degradation mechanisms of the multistage PID, on the basis of the obtained results.

2. Experimental procedure

20 × 20-mm^2-sized n-type FE c-Si PV cells with Si nitride (SiN_x)/Si dioxide (SiO_2) passivation stacks were prepared into mini modules by using a laminator. The lamination process used in this study was the same as that used in a previous study [18]. The modules were composed of conventional tempered cover glass/ethylene-vinyl acetate copolymer (EVA) encapsulant/cell/EVA encapsulant/typical backsheet. The size of the cover glass was 45 × 45 mm^2 and contained alkali metals such as Na. The EVA encapsulants had a relatively low volume resistance of 1.5 × 10^{15} Ω·cm. The backsheets were composed of polyvinyl fluoride (PVF)/polyethylene terephthalate (PET)/PVF.

PID tests were performed by applying a negative bias of −1000 V to shorted interconnector ribbons of the modules with respect to an Al plate placed on the cover glass surface at a temperature of 85 °C and a relative humidity of <2%, for up to 20 days in total. The PID tests were performed for three identical modules on each condition. After confirming the degradation by the PID tests, recovery tests were performed by applying a positive bias of +1000 V to the cells with respect to the Al plate placed on the cover glass surface at a temperature of 85 °C and a relative humidity of <2%. The recovery tests were conducted on the modules degraded by the PID tests for 120 s, 12 h, and 480 h. The durations of the recovery tests were the same as those of the degradation tests. A recovery test under each condition was performed on one module. The same PID test was also performed using a module containing a commercial size cell with an area of 156 × 156 mm^2 for comparison. To ensure contact between the Al plate and the cover glass, an electrically conductive rubber sheet was inserted between them.

To evaluate the performance degradation, dark and one-sun-illuminated current density–voltage (*J–V*), and external quantum efficiency (EQE) measurements were performed before and after the PID tests and recovery tests. From these results, the J_{sc}, V_{oc}, FF, and maximum power (P_{max}) values were obtained. We obtained the results by ex-situ measurements. After taking out PV modules from the test chamber, we performed dark and one-sun-illuminated *J–V* measurements, EQE measurements on the modules. The measured dark *J–V* data before and after the PID tests were fitted to the two-diode equation [24], to obtain the saturation current densities J_{01} and J_{02} of the first and second diodes, respectively, the ideality factors n_1 and n_2 of the first and second diodes, respectively, the R_p, and the series resistances R_s. In the two-diode fitting, n_1 was restricted to one, and n_2 was limited to greater than one, J_{01}, J_{02}, R_p and R_s were positive. Additionally, we assumed that the R_s of the modules after degradation was not lower than that of the initial modules. Dark *J–V* characteristics are expressed by the following equation:

$$J(V) = J_{01}\left[\exp\left(\frac{q(V-JR_s)}{n_1 kT}\right)-1\right] + J_{02}\left[\exp\left(\frac{q(V-JR_s)}{n_2 kT}\right)-1\right] + \frac{V-JR_s}{R_p}, \quad (1)$$

where q is the elementary charge, k the Boltzmann constant, and T the absolute temperature.

3. Results

3.1 Degradation behavior in long-term PID tests

The PID of n-type FE PV modules is known to rapidly occur and to saturate within a quite a short time, for instance several minutes. So far, most researchers have mainly dealt with the initial-stage degradation, and behavior after the initial-stage degradation has not yet been investigated in detail. In this study, through the rapid PID test method, we investigated the degradation behavior of n-type c-Si PV modules in PID tests with a long duration of up to 20 days.

Fig. 1 shows the PID-stress duration dependence of $J_{sc}/J_{sc,0}$, $V_{oc}/V_{oc,0}$, FF/FF$_0$ and $P_{max}/P_{max,0}$, where the subscript 0 indicates the initial value. After the PID tests applying a negative bias of −1000 V, the J_{sc} and the V_{oc} started to decrease within 10 s and strongly saturated within approximately 120 s, resulting in a reduction in the P_{max} and its saturation. This rapid degradation has been reported to be attributed to additional positive-charge accumulation in the front SiN_x passivation layers [16,17,19]. After the saturation, all the parameters were almost unchanged until after 1 h. However, the FF then started to decrease and saturated again. After approximately 48 h, the FF further decreased again, accompanied by a reduction in the V_{oc}. This result demonstrates that the n-type c-Si PV modules undergo three-stage degradations: rapid reductions in the V_{oc} and the J_{sc}, a reduction in the FF, and a reduction in the FF accompanied by a decrease in the V_{oc}.

Figs. 2 and 3 show the dark J–V curves of the PV modules before and after PID tests and the J_{01}, the J_{02}, the n_2 and 1000/R_p as a function of PID-stress duration. The J_{01} increased within about 10 s and strongly saturated within 120 s, implying an enhancement in bulk and/or surface recombination and its saturation. These coincided with the first degradation which was caused by reductions in the V_{oc} and the J_{sc}. This J_{01} increase has been reported to be attributed to enhanced surface recombination caused by positive-charge accumulation in the front SiN_x passivation layers [16,17,19]. An enhancement in surface recombination can be confirmed as a reduction in EQE in a short-wavelength range, as shown in Fig. 4.

After the saturation of the J_{01}, the J_{02} and the n_2 started to increase and saturated after approximately 3h. These increases in the J_{02} and the n_2 simultaneously occurred with the second degradation, which is characterized by a reduction in the FF. Increases in the J_{02} and the n_2 generally indicate an enhancement in recombination in the space charge region. This result therefore suggests that the second degradation is related to enhanced recombination in the space charge region. As can be seen in Fig. 4, the second

degradation is not accompanied by a reduction in EQE.

$1000/R_p$ gradually increased from 2 h and further noteworthy increased from 96 h. The J_{02} and the n_2 also significantly increased again from 96 h to 480 h. These phenomena characterized the third degradation. Note that the increase in $1000/R_p$ was accompanied by a superlinear reverse bias characteristic in the dark *J–V* curves, as shown in Fig. 2(b). This characteristic behavior of the dark *J–V* curves may be a key to explain the degradation mechanism. Deviations between the fitting results and the measured *J–V* data became larger owing to the superlinear characteristics. To obtain better fitting results, another term may have to be considered. In this study, we used the typical two-diode model equation for fitting the data; in addition, we will discuss the origin of the superlinear characteristics based on the temperature dependence of reverse bias currents and some previous studies.

3.2 Recovery behavior

It is well known that the PID of p-type c-Si [2,25], n-type c-Si [17,20] and CIGS [26] solar cells recover when a reverse bias is applied to a module degraded by PID tests. We investigated whether the degradation of n-type FE c-Si PV modules on each stage can be recovered by applying a positive bias of +1000 V. Figs. 5, 6, and 7 show the one-sun-illuminated and dark *J–V* curves of n-type FE c-Si PV modules before and after PID tests and after recovery tests for the pre-degraded module. The durations of the PID tests were 120 s, 12 h, and 480 h, which correspond to the first, second, and third degradation stages, respectively. The durations of recovery tests were set to the same as those of the prior degradation tests.

After the PID test for 120 s, the module showed the first degradation characterized by reductions in the V_{oc} and the J_{sc} which were accompanied by an increase in the J_{01}. As shown in Fig. 5(a), the module recovered its performance loss characterized by the reductions in the V_{oc} and the J_{sc}. The J_{01} was also completely recovered (Fig. 5(b)). This demonstrates that the first degradation of n-type FE c-Si PV module can be readily recovered. This recovery process can be explained by the detrapping of positive charges accumulating in the front SiN_x layer [17].

After the PID and recovery test for 12 h, respectively, all the parameters were almost completely recovered; however, a slight reduction in the FF remained, as shown in Fig 6(a). This appears to be caused by a slight increase in the J_{02} which remained even after the recovery test (Fig. 6(b)). On the contrary, the J_{sc} and the V_{oc} were not recovered at all, and only slight recovery in the FF was observed after the PID and successive recovery tests for 480 h, respectively, as shown in Fig. 7(a). This slight recovery was caused by that of the J_{02} (Fig. 7(b)). These results suggest that the degree of performance recovery strongly depends on that of degradation. A similar trend has been reported in PID in conventional p-type c-Si PV modules [25].

4. Discussion

4.1 Degradation behavior in long-term PID tests

In this work, we investigated the progression behavior of the PID of n-type c-Si PV modules, by using PID tests with a long duration of up to 20 days. We found that the n-type FE c-Si PV modules underwent multistage degradations divided into three stages as shown in Fig. 1.

The first degradation was characterized by rapid reductions in the J_{sc} and the V_{oc}, which were accompanied by an increase in the J_{01} and a significantly reduced EQE in a short wavelength range, and exhibited rapid saturation of their variations. The degradation is known to be caused by the accumulation of additional positive charges in the front SiN_x passivation layers [16,17,19]. As for the saturation behavior, we have proposed a mechanism that the saturation is due to a positive-charge density limited by the density of K centers present in the front SiN_x passivation films [17].

The second degradation was characterized by reduction in the FF. This may be caused by an increase in recombination in the space charge region. This assumption is supported by the increased J_{02} and n_2. The modules with the second degradation showed significant increases in J_{02} and n_2 after the PID test for 12 h. As can be seen in Fig. 3, the second degradation was not accompanied by a significant reduction in the R_p. This suggests that the second degradation is related not to the (linear) shunting of the p–n junctions but to enhanced recombination in the space charge region. The enhancement in recombination in the space charge region may be due to space charge region recombination via defect levels formed by Na atoms introduced into the space charge region through the cell edges and/or the front SiN_x passivation layers. Similar behavior has been reported on PID in n-type c-Si PV modules with a glass/glass structure, in which it has been suggested that a reduction in the FF may be attributed to an increase in recombination in the space charge region [23].

The third degradation was characterized by reductions in the FF and the V_{oc}. This may be caused by a further increase in recombination in the space charge region and significant reduction in the R_p. As can be seen in Fig. 3, the J_{02} and the n_2 further increased from 96 h to 480 h in the PID test, which shows the similar behavior to the second degradation. However, $1000/R_p$ in Fig. 3 significantly increased from 96 h to 480 h in the PID test, which is different from the second degradation. As for the PID of the p-type c-Si PV modules, a reduction in the R_p is known to be caused by the shunting of the p–n junctions [8]. However, the dark *J–V* curve of our PV modules after the PID tests for 480 h in Fig. 2(b) shows a superlinear behavior on the reverse bias side, which implies that the observed decreased R_p is based on a mechanism different from that of the shunting observed in p-type c-Si PV modules. This reverse-bias superlinear behavior might be due to introduced impurities such as Na atoms that are considered to provide many defect levels in the space charge regions. It is well known that when multiple impurity levels are introduced into the space charge regions, similar superlinear

reverse-bias currents are observed [27,28]. Additionally, the reverse-bias currents are known to show positive temperature coefficients. In order to test our assumption, we investigated the temperature dependence of the reverse-bias current density. The result is shown in Fig. 8, where the module showed superlinear reverse-bias current after the PID test for 480 h. The reverse-bias current appears to increase as the temperature rises. This positive temperature coefficient of the reverse-bias current is not inconsistent with the assumption that the reverse-bias superlinear characteristics are caused by many defect levels introduced into the space charge regions. This kind of superlinear characteristic is known to be observed for example when the precipitates of metal impurities are formed [27]. This implies that a very large amount of impurities were introduced into the space charge regions of our cells by the PID stress.

We confirmed that there is no degradation just by storing modules at a temperature of 85 °C for 480 h (not shown here), suggesting that the observed degradation is due to the negative bias application.

Note that there is a possibility that the effect of Na atoms introduced into the space charge region strongly appeared because our small cells have unpassivated cell edges. In our cells, Na probably tends to be easily introduced through the cell edges, which leads to the overestimation of the effect of Na. Additionally, our cells were small (20 × 20-mm^2-sized), which may lead to the overestimation of the edge recombination in the space charge region. We therefore compared the results of small-sized modules with a module with a full-sized cell one. The FF started to decrease after approximately 1 h in the small-sized modules. The FF started to decrease also in the module with a full-sized cell after approximately 12 h. This indicates that the decrease in the FF is not limited to the small-sized modules, although the unpassivated cell edges may partly affect the emergence of degradation in the FF. Furthermore, the V_{oc} and the FF of the small and modules with a full-sized cell decreased with a similar time dependence to the same degree from after approximately 48 h (not shown here). From this result, it is suggested that the PID of n-type FE c-Si PV modules observed in this work could also occur in large-scale PV systems.

4.2 Recovery behavior

By performing the recovery tests on the modules with the first, second, and third degradations, we found that the module with the first and second degradations almost completely recovered their performance losses. On the other hand, the module with the third degradation could not be recovered. This suggests that the recovery behavior strongly depends on the degree of degradation. For the module with the first degradation, its recovery behavior has been reported to be explained as a positive-charge detrapping process, in a previous study [17]. In this section, we therefore discuss the recovery behavior of PV modules with the second and third degradations.

The almost complete recovery of the second degradation may be due to the

detrapping of positive charges accumulating in the front SiN_x passivation layers mentioned above and the out-diffusion of Na that is introduced into the space charge region in the p–n junction. The dark *J–V* curves (Fig. 6(b)) show that the J_{01} was completely recovered after the PID recovery test for 12 h, leading to complete recoveries in the J_{sc} and the V_{oc}. This result was due to the detrapping of positive charges accumulating in the front SiN_x passivation layers. On the other hand, the J_{02} and the n_2 were partly recovered, leading to a partly recovered FF. On the basis of the above discussion (Sect. 4.1), the second degradation is caused by Na atoms introduced into the space charge region; therefore, we considered the recovery to be associated with the out-diffusion of Na from the space charge region at present.

The slight recovery of the third degradation might be due to the partial out-diffusion of Na atoms. Na atoms near the cell surface could diffuse out from the c-Si during the recovery tests, while Na atoms that have diffused deep into the c-Si may remain, since the electric field between the Al plate on the module surface and the cell electrodes does not affect inside the c-Si. These remaining Na atoms may limit the performance of n-type FE c-Si PV modules and lead to the unrecoverable phenomenon.

5. Conclusions

We investigated the behavior of the performance of the n-type FE c-Si PV modules in the PID tests with a long duration of up to 20 days. We found that the modules underwent three-stage degradations. The first degradation was characterized by rapid reductions in the J_{sc} and the V_{oc}. This is known to be caused by the accumulation of positive charges in the front SiN_x passivation layers. The second degradation was characterized by reductions in the FF. This may be caused by an increase in recombination in the space charge region. The third degradation was characterized by reductions in the FF and the V_{oc}. This may be caused by a further increase in recombination in the space charge region and significant reduction in the R_p. The second and third degradations may be due to space charge region recombination via many defect levels formed by Na atoms introduced into the space charge region in the p–n junction through the cell edges and/or the front SiN_x passivation layers.

We also investigated whether the degradation on each stage can be recovered by applying a positive bias of +1000 V. The module with the first degradation completely recovered its performance losses, and the module with the second degradation was almost completely recovered. The module with the third degradation could not almost be recovered. This suggests that the degree of performance recovery strongly depends on that of degradation. For the module with the first degradation, its recovery behavior has been reported to be explained as a positive-charge detrapping process. The almost complete recovery of the second degradation may be due to the detrapping of positive charges accumulating in the front SiN_x passivation layers and the out-diffusion of Na that is introduced into the space charge region in the p–n junction. The slight recovery of the

third degradation might also be due to the out-diffusion of a part of Na atoms.

Acknowledgments

This work was supported by the New Energy and Industrial Technology Development Organization (NEDO) and JSPS KAKENHI Grant Number JP17J09648.

References

[1] W. Luo, Y.S. Khoo, P. Hacke, V. Naumann, D. Lausch, S.P. Harvey, J.P. Singh, J. Chai, Y. Wang, A.G. Aberle, S. Ramakrishna, Potential-induced degradation in photovoltaic modules: a critical review, Energy Environ. Sci. 10 (2017) 43–68.

[2] S. Pingel, O. Frank, M. Winkler, S. Daryan, T. Geipel, H, Hoehne, J. Berghold, Potential induced degradation of solar cells and panels, in: Proceedings of 35th IEEE Photovoltaic Specialists Conference, 20–25 June, Honolulu, HI, USA, 2010, pp. 2817–2822.

[3] J. Berghold, O. Frank, H. Hoehne, S. Pingel, B. Richardson, M. Winkler, Potential induced degradation of solar cells and panels, In: Proceedings of the 25th European Photovoltaic Solar Energy Conference and Exhibition/5th World Conference on Photovoltaic Energy Conversion, 6–10 September, Valencia, Spain, 2010, pp. 3753–3759.

[4] P. Hacke, M. Kempe, K. Terwilliger, S. Glick, N. Call, S. Johnston, S. Kurtz, I. Bennett, M. Kloos, Characterization of multicrystalline silicon modules with system bias voltage applied in damp heat, In: Proceedings of the 25th European Photovoltaic Solar Energy Conference and Exhibition/5th World Conference on Photovoltaic Energy Conversion, 6–10 September, Valencia, Spain, 2010, pp. 3760–3765.

[5] J. Bauer, V. Naumann, S. Großer, C. Hagendorf, M. Schütze, O. Breitenstein, On the mechanism of potential-induced degradation in crystalline silicon solar cells, Phys. Status Solidi: Rapid Res. Lett. 6 (2012) 331–333.

[6] V. Naumann, C. Hagendorf, S. Grosser, M. Werner, J. Bagdahn, Micro structural root cause analysis of potential induced degradation in c-Si solar cells, Energy Procedia 27 (2012) 1–6.

[7] V. Naumann, D. Lausch, C. Hagendorf, Sodium decoration of PID-s crystal defects after corona induced degradation of bare silicon solar cells, Energy Procedia 77 (2015) 397–401.

[8] V. Naumann, D. Lausch, A. Hähnel, J. Bauer, O. Breitenstein, A. Graff, M. Werner, S. Swatek, S. Großer, J. Bagdahn, C. Hagendorf, Explanation of potential-induced degradation of the shunting type by Na decoration of stacking faults in Si solar cells, Sol. Energy Mater. Sol. Cells 120 (2014) 383–389.

[9] V. Naumann, C. Brzuska, M. Werner, S. Großer, C. Hagendorf, Investigations on the formation of stacking fault-like PID-shunts, Energy Procedia 92 (2016) 569–575.

[10] M. Wilson, A. Savtchouk, P. Edelman, D. Marinskiy, J. Lagowski, Drift characteristics of mobile ions in SiN_x films and solar cells, Sol. Energy Mater. Sol. Cells 142 (2015) 102–106.

[11] J.W. Osenbach, S.S. Voris, Sodium diffusion in plasma-deposited amorphous oxygen-doped silicon nitride (a-SiON:H) films, J. Appl. Phys. 63 (1988) 4494–4500.

[12] A. ur Rehman, S.H. Lee, Advancements in n-type base crystalline silicon solar cells and their emergence in the photovoltaic industry, Sci. World J. 2013 (2013) 470347.

[13] R. Swanson, M. Cudzinovic, D. DeCeuster, V. Desai, J. Jürgens, N. Kaminar, W. Mulligan, L. Rodrigues-Barbosa, D. Rose, D. Smith, A. Terao, K. Wilson, The surface polarization effect in high-efficiency silicon solar cells, in: Technical Digest of the 15th Photovoltaic Science and Engineering Conference, 10–15 October, Shanghai, China, 2005, pp. 410–411.

[14] V. Naumann, T. Geppert, S. Großer, D. Wichmann, H.-J. Krokoszinski, M. Werner, C. Hagendorf, Potential-induced degradation at interdigitated back contact solar cells, Energy Procedia 55 (2014) 498–503.

[15] A. Halm, A. Schneider, V.D. Mihailetchi, L.J. Koduvelikulathu, L.M. Popescu, G. Galbiati, H. Chu, R. Kopecek, Potential-induced degradation for encapsulated n-type IBC solar cells with front floating emitter, Energy Pocedia 77 (2015) 356–363.

[16] K. Hara, S. Jonai, A. Masuda, Potential-induced degradation in photovoltaic modules based on n-type single crystalline Si solar cells, Sol. Energy Mater. Sol. Cells 140 (2015) 361–365.

[17] S. Yamaguchi, A. Masuda, K. Ohdaira, Progression of rapid potential-induced degradation of n-type single-crystalline silicon photovoltaic modules, Appl. Phys. Express 9 (2016) 112301.

[18] S. Yamaguchi, A. Masuda, K. Ohdaira, Changes in the current density-voltage and external quantum efficiency characteristics of n-type single-crystalline silicon photovoltaic modules with a rear-side emitter undergoing potential-induced degradation, Sol. Energy Mater. Sol. Cells 151 (2016) 113–119.

[19] S. Bae, W. Oh, K. D. Lee, S. Kim, H. Kim, N. Park, S.-I. Chan, S. Park, Y. Kang, H-S. Lee, D. Kim, Potential induced degradation of n-type crystalline silicon solar cells with p^+ front junction, Energy Sci. Eng. 5 (2017) 30–37.

[20] M. Barbato, A. Barbato, M. Meneghini, G. Tavernaro, M. Rossetto, G. Meneghesso, Potential induced degradation of N-type bifacial silicon solar cells: An investigation based on electrical and optical measurements, Sol. Energy Mater. Sol. Cells 168 (2017) 51–61.

[21] K. Hara, K. Ogawa, Y. Okabayashi, H. Matsuzaki, A. Masuda, Influence of surface structure of n-type single-crystalline Si solar cells on potential-induced degradation, Sol. Energy Mater. Sol. Cells 166 (2017) 132–139.

[22] S. Yamaguchi, C. Yamamoto, K. Ohdaira, A. Masuda, Reduction in the short-circuit current density of silicon heterojunction photovoltaic modules subjected to potential-induced degradation tests, Sol. Energy Mater. Sol. Cells 161 (2017) 439–443.

[23] W. Luo, Y.S. Khoo, J.P. Singh, J.K.C. Wong, Y. Wang, A.G. Aberle, S. Ramakrishna,

Investigation of Potential-Induced Degradation in n-PERT Bifacial Silicon Photovoltaic Modules with a Glass/Glass Structure, IEEE J. Photovoltaics 8 (2018) 16–22.

[24] M. Wolf, G.T. Noel, R.J. Stirn, Investigation of the double exponential in the current-voltage characteristics of silicon solar cells, IEEE Trans. Electron Devices 24 (1977) 419–428.

[25] A. Masuda, M. Akitomi, M. Inoue, K. Okuwaki, A. Okugawa, K. Ueno, T. Yamazaki, K. Hara, Microscopic aspects of potential-induced degradation phenomena and their recovery processes for p-type crystalline Si photovoltaic modules, Curr. Appl. Phys. 16 (2016) 1659–1665.

[26] S. Yamaguchi, S. Jonai, K. Hara, H. Komaki, Y. Shimizu-Kamikawa, H. Shibata, S. Niki, Y. Kawakami, A. Masuda, Potential-induced degradation of Cu(In,Ga)Se_2 photovoltaic modules, Jpn. J. Appl. Phys. 54 (2015) 08KC13.

[27] K. Bothe, K. Ramspeck, D. Hinken, C. Schinke, J. Schmidt, S. Herlufsen, R. Brendel, J. Bauer, J.-M. Wagner, N. Zakharov, O. Breitenstein, Luminescence emission from forward- and reverse-biased multicrystalline silicon solar cells, J. Appl. Phys. 106 (2009) 104510.

[28] O. Breitenstein, J. Bauer, K. Bothe, W. Kwapil, D. Lausch, U. Rau, J. Schmidt, M. Schneemann, M.C. Schubert, J.-M. Wagner, W. Warta, Understanding junction breakdown in multicrystalline solar cells, J. Appl. Phys. 109 (2011) 071101.

Figure Captions

Fig. 1. PID-stress duration dependence of the performance of the n-type FE c-Si PV modules undergoing the PID tests applying −1000 V. Each data point shows the mean value for the three modules, and each error bar corresponds to the standard deviation of the mean. The solid lines are included as guides for the eye.

Fig. 2. Dark *J–V* curves of the n-type FE c-Si PV modules before and after the PID tests for 120 s, 12 h and 480 h. (a) is on a log scale and (b) is on a linear scale.

Fig. 3. PID-stress-duration dependence of the J_{01}, the J_{02}, the n_2 and $1000/R_p$ of the n-type FE c-Si PV modules undergoing the PID tests in which a negative bias of −1000 V was applied. Each data point shows the mean value for the three modules, and each error bar corresponds to the standard deviation of the mean. The solid lines are included as guides for the eye.

Fig. 4. EQE spectra of the n-type FE c-Si PV modules before and after the PID tests applying −1000 V for 120 s and 480 h.

Fig. 5. (a) One-sun-illuminated and (b) dark *J–V* curves of the n-type FE c-Si PV modules before and after the PID tests in which a negative bias of −1000 V was applied for 120 s and after the subsequent PID recovery test applying +1000 V for 120 s.

Fig. 6. (a) One-sun-illuminated and (b) dark *J–V* curves of the n-type FE c-Si PV modules before and after the PID tests in which a negative bias of −1000 V was applied for 12 h and after the subsequent PID recovery test applying +1000 V for 12 h.

Fig. 7. (a) One-sun-illuminated and (b) dark *J–V* curves of the n-type FE c-Si PV modules before and after the PID tests in which a negative bias of −1000 V was applied for 480 h and after the subsequent PID recovery test applying +1000 V for 480 h.

Fig. 8. Temperature-dependent reverse-bias dark *J–V* characteristics of the n-type FE c-Si PV modules.

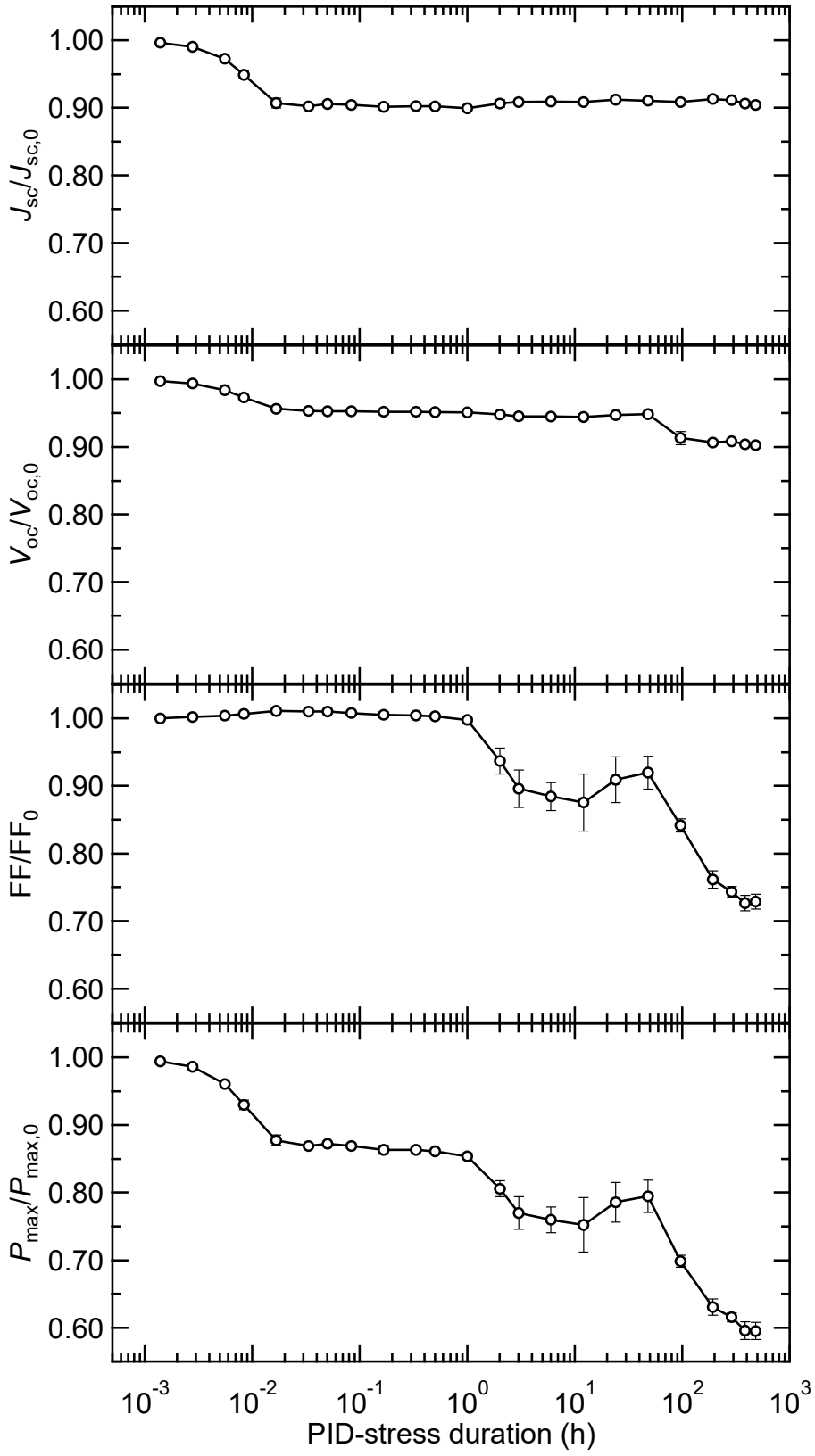
1.00
0.90
0.80
0.70
0.60
$J_{sc}/J_{sc,0}$
$V_{oc}/V_{oc,0}$
FF/FF_0
$P_{max}/P_{max,0}$
10^{-3}
10^{-2}
10^{-1}
10^{0}
10^{1}
10^{2}
10^{3}
PID-stress duration (h)

Fig. 1

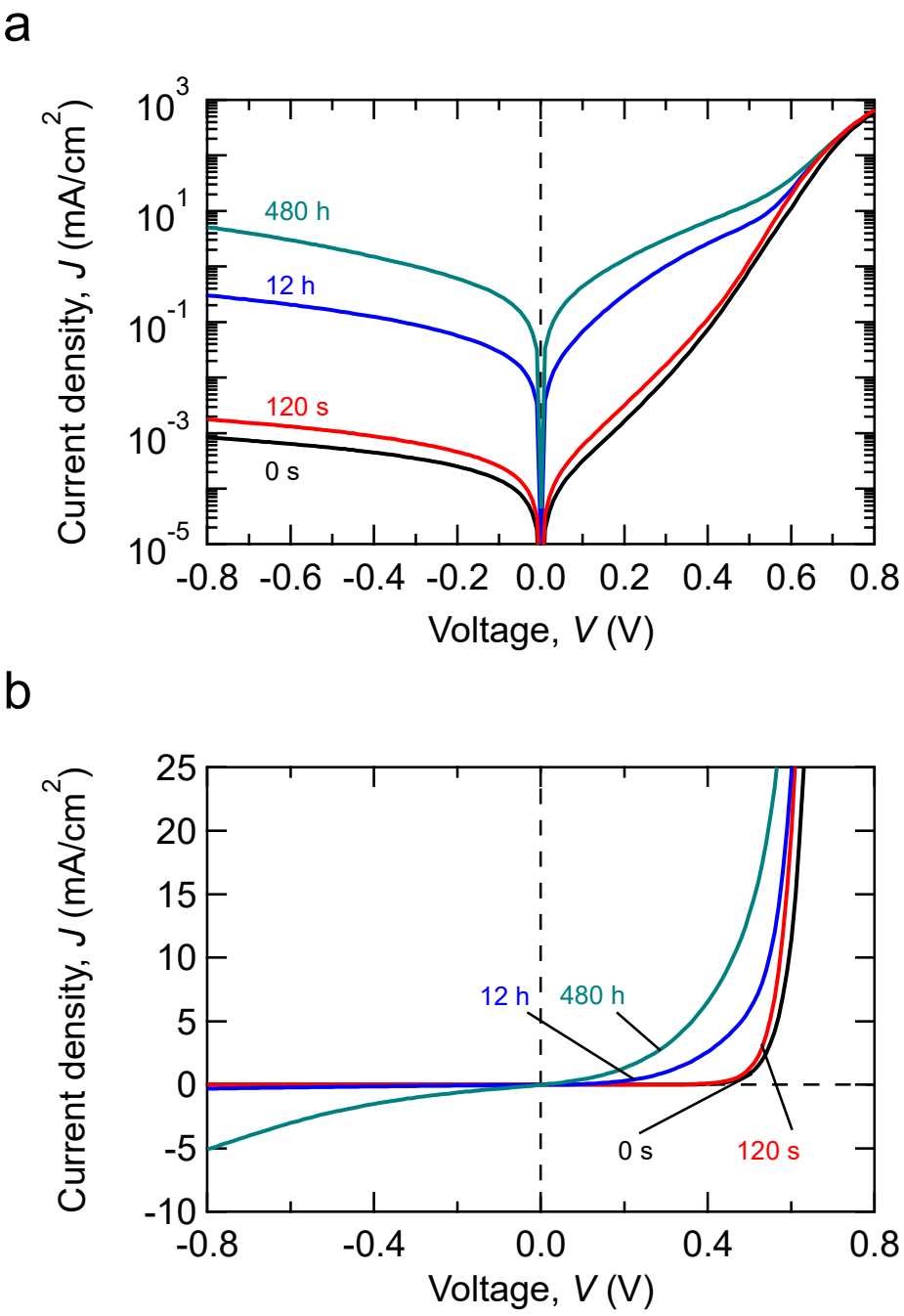
a
Current density, J (mA/cm2)
10^3
10^1
10^-1
10^-3
10^-5
480 h
12 h
120 s
0 s
-0.8 -0.6 -0.4 -0.2 0.0 0.2 0.4 0.6 0.8
Voltage, V (V)
b
Current density, J (mA/cm2)
25
20
15
10
5
0
-5
-10
12 h
480 h
0 s
120 s
-0.8 -0.4 0.0 0.4 0.8
Voltage, V (V)

Fig. 2

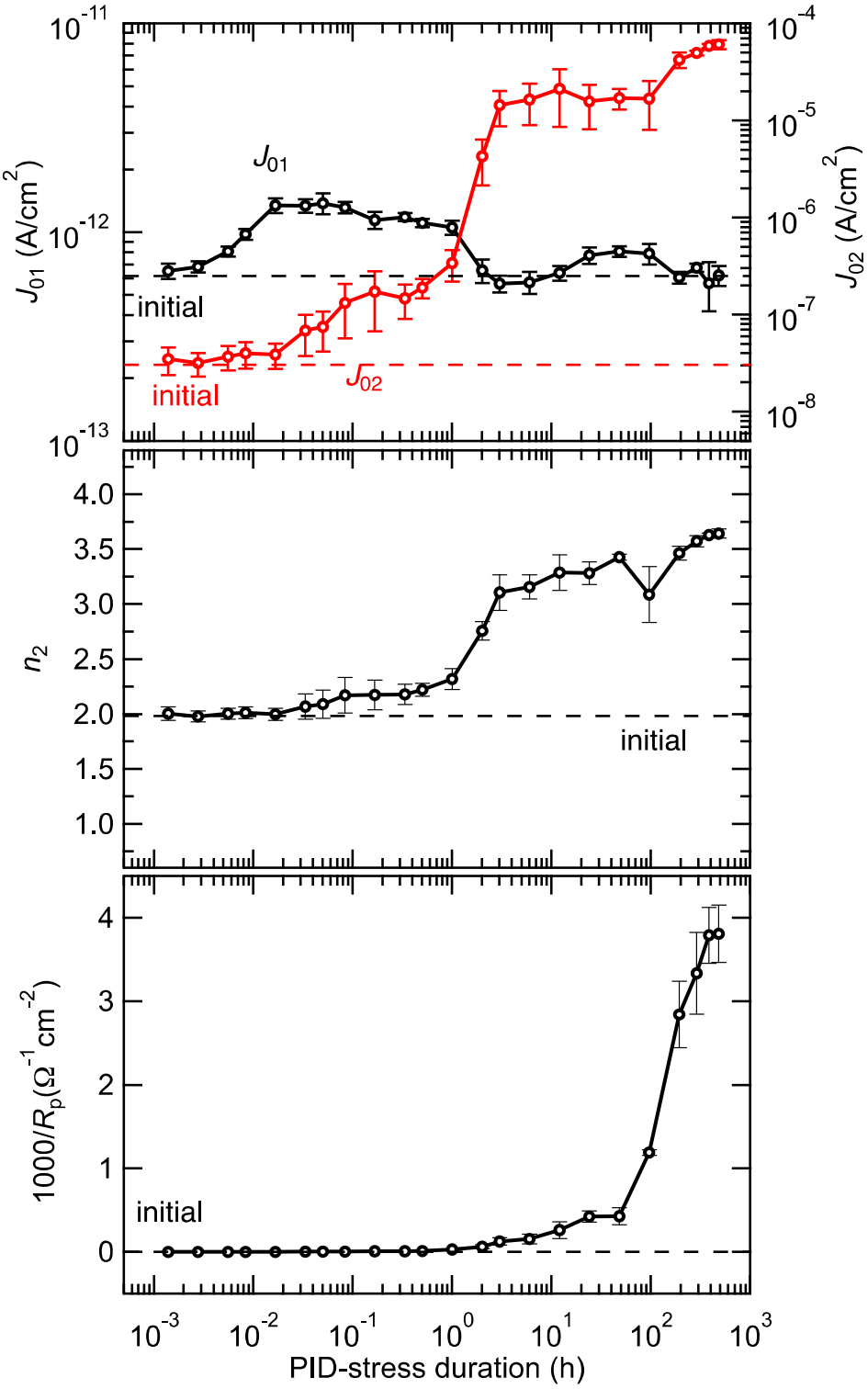
J_{01} (A/cm^2)
J_{02} (A/cm^2)
J_{01}
initial
J_{02}
initial
n_2
initial
1000/R_p(Ω^{-1}cm^{-2})
initial
PID-stress duration (h)

Fig. 3

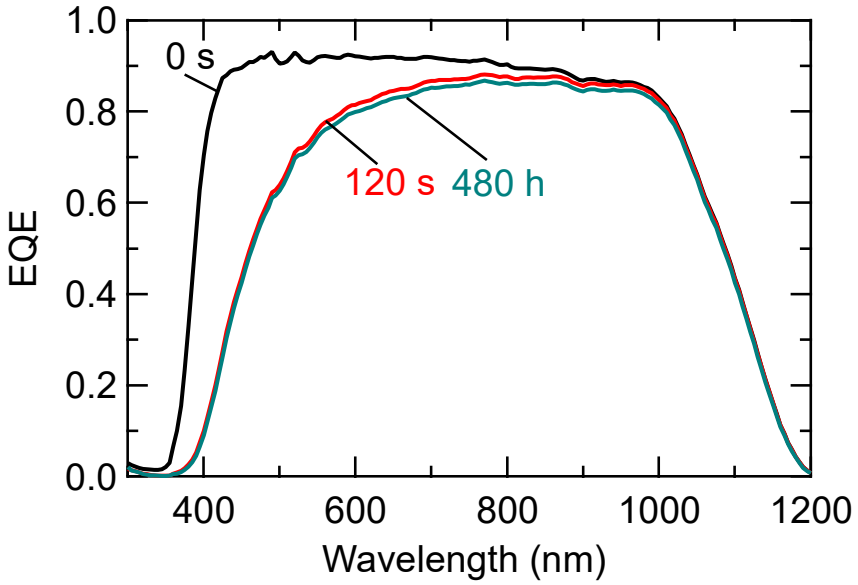
1.0
0.8
0.6
0.4
0.2
0.0
EQE
0 s
120 s
480 h
400
600
800
1000
1200
Wavelength (nm)

Fig. 4

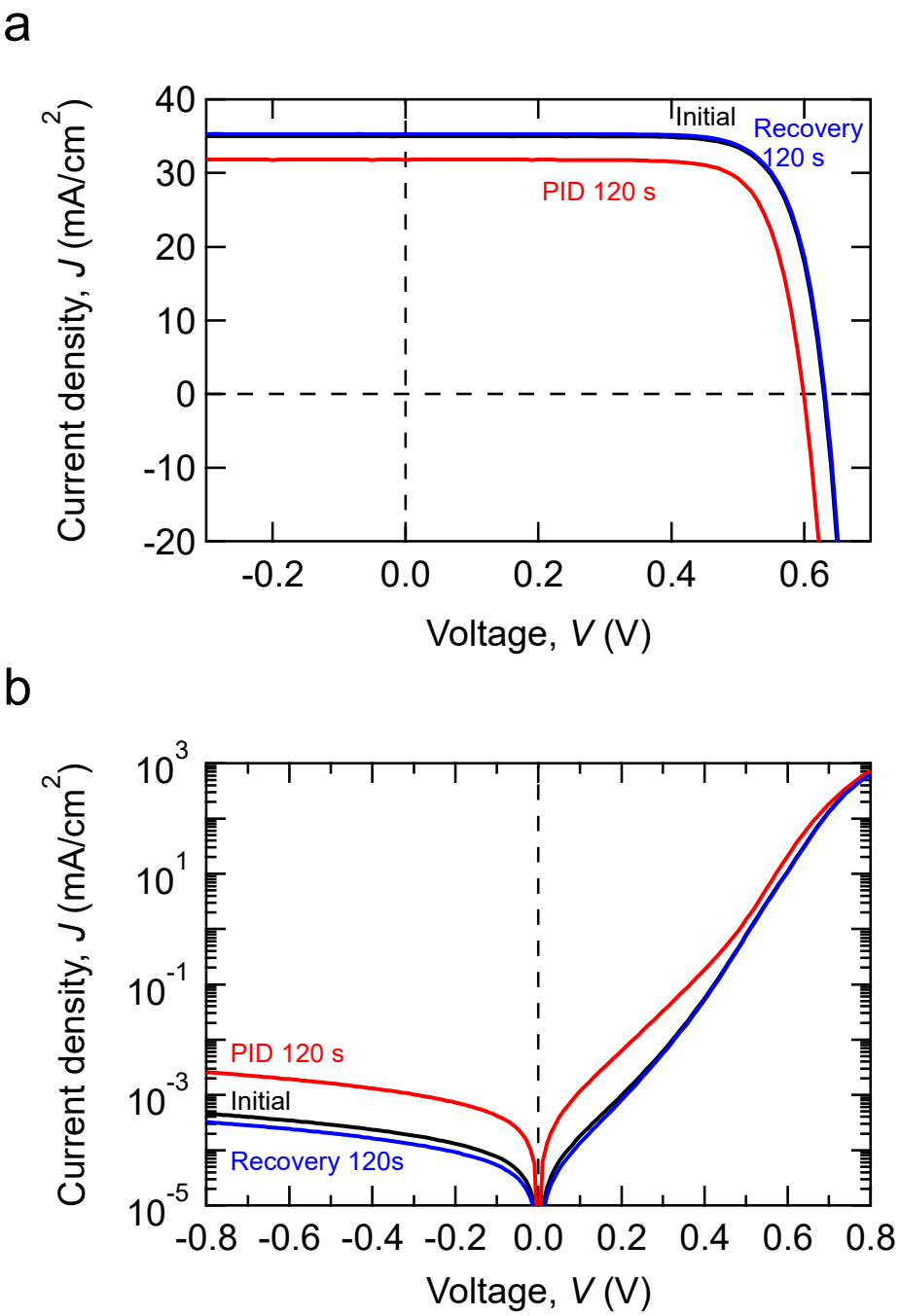
a
Initial
Recovery
120 s
PID 120 s
Current density, J (mA/cm2)
Voltage, V (V)
b
PID 120 s
Initial
Recovery 120s
Current density, J (mA/cm2)
Voltage, V (V)

Fig. 5

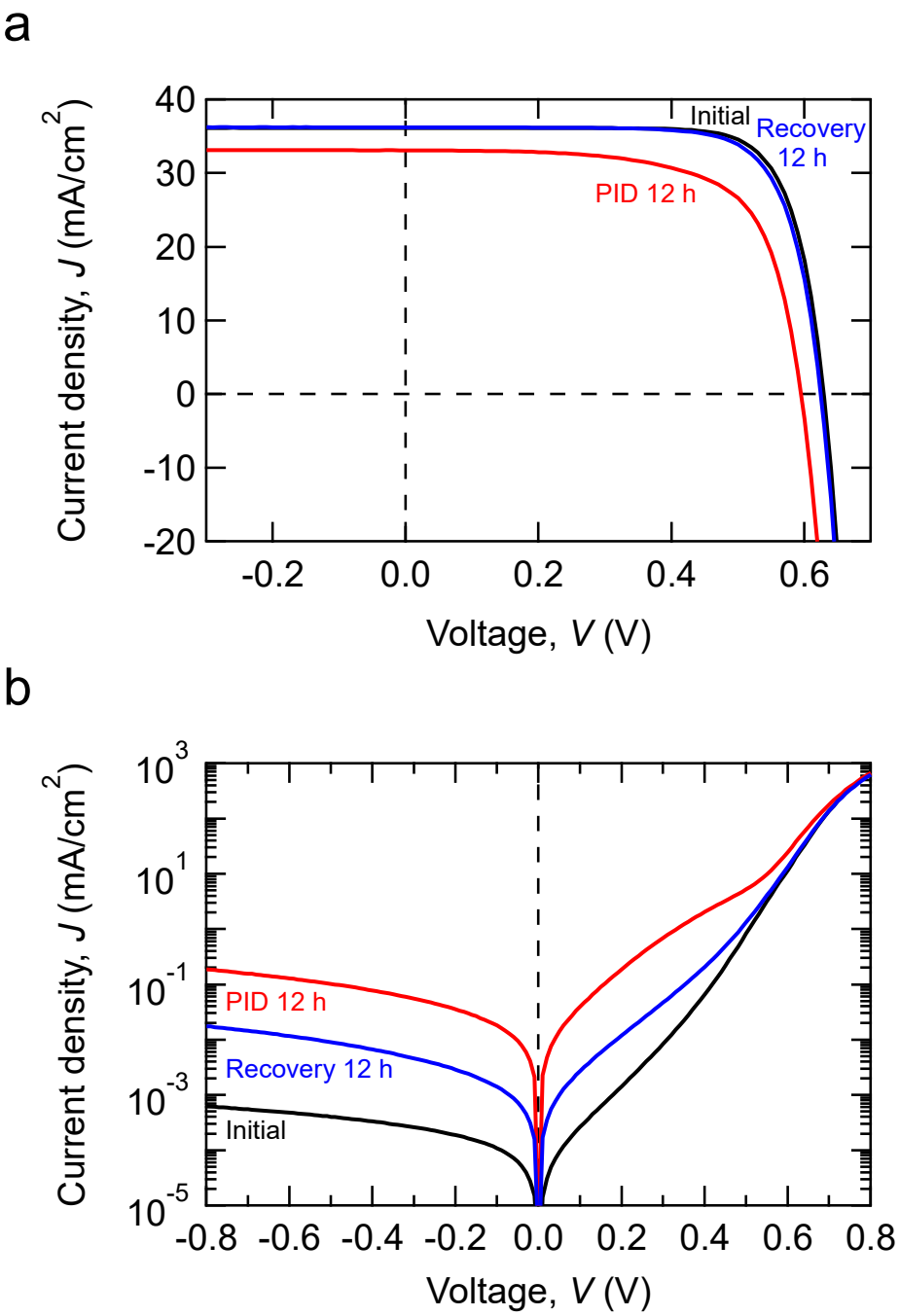
a
Current density, J (mA/cm2)
Voltage, V (V)
Initial
Recovery 12 h
PID 12 h
40
30
20
10
0
-10
-20
-0.2
0.0
0.2
0.4
0.6
b
Current density, J (mA/cm2)
Voltage, V (V)
PID 12 h
Recovery 12 h
Initial
10^3
10^1
10^-1
10^-3
10^-5
-0.8
-0.6
-0.4
-0.2
0.0
0.2
0.4
0.6
0.8

Fig. 6

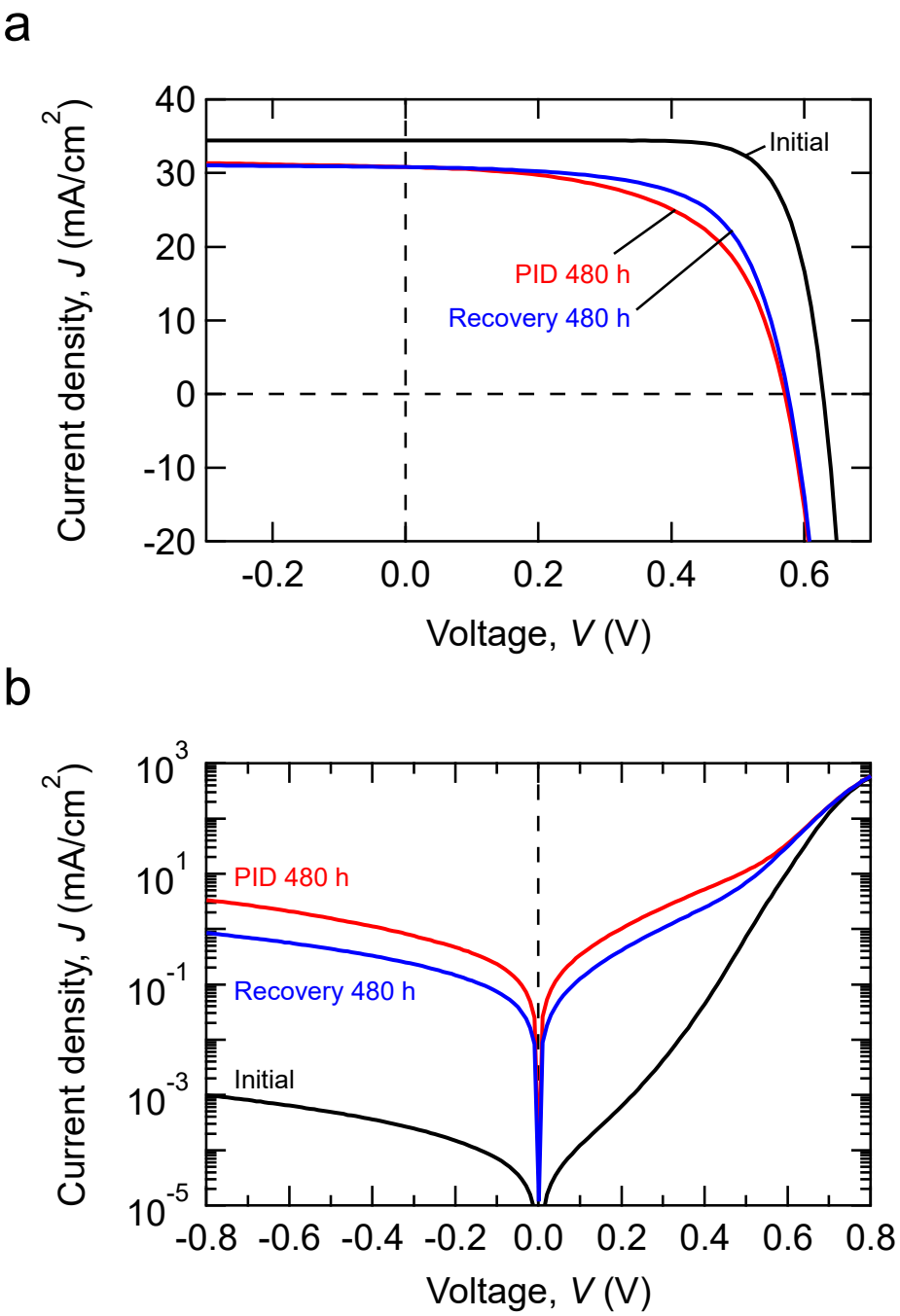
a
Current density, J (mA/cm2)
40
30
20
10
0
-10
-20
-0.2
0.0
0.2
0.4
0.6
Voltage, V (V)
Initial
PID 480 h
Recovery 480 h
b
Current density, J (mA/cm2)
10^3
10^1
10^-1
10^-3
10^-5
-0.8
-0.6
-0.4
-0.2
0.0
0.2
0.4
0.6
0.8
Voltage, V (V)
PID 480 h
Recovery 480 h
Initial

Fig. 7

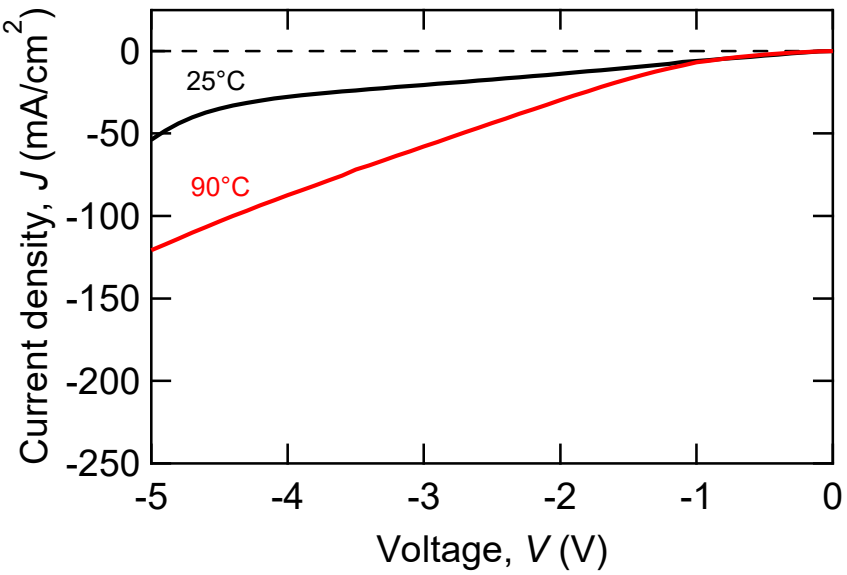
Current density, J (mA/cm2)
0
-50
-100
-150
-200
-250
25°C
90°C
-5
-4
-3
-2
-1
0
Voltage, V (V)

Fig. 8